Available online at www.derpharmachemica.com

ISSN 0975-413X
CODEN (USA): PCHHAX

Der Pharma Chemica, 2016, 8(2):256-268
(http://derpharmachemica.com/archive.html)

The inhibition performance of sulfamerazine for corrosion of mild steel in HCl

B. El Makrini[1], H. Lgaz[1,2], M. Larouj[2], R. Salghi[1*], A. Rasem Hasan[3,*], M. Belkhaouda[1], S. Jodeh[4], M. Zougagh[5,6] and H. Oudda[2]

[1]*Laboratory of Applied Chemistry and Environment, ENSA, Université Ibn Zohr, Agadir, Morocco*
[2]*Laboratory separation processes, Faculty of Science, University Ibn Tofail, Kenitra, Morocco*
[3]*Department of Civil Engineering, An-Najah National University, Nablus, Palestine*
[4]*Department of Chemistry, An-Najah National University, Nablus, Palestine*
Laboratory of Organic, Organometallic and Theoretical Chemistry, Faculty of Science, Ibn Tofaïl University, Kenitra, Morocco
[5]*Regional Institute for Applied Chemistry Research, IRICA, E-13004, Ciudad Real, Spain*
[6]*Castilla-La Mancha Science and Technology Park, E-02006, Albacete, Spain*

ABSTRACT

The corrosion inhibition characteristics of Sulfamerazine(SFM) on mild steel immersed in 1 M HCl solution were investigated. Weight loss, electrochemical impedance spectroscopy (EIS), potentiodynamic polarisation (PDP) was used as basis for studying the corrosion inhibition behavior of the compound. The results show that the inhibition efficiency increase with increase in SFM concentration in the acidic solutions but decreases with increase in temperature. Specifically. Langmuir isotherm best fits the data obtained suggesting chemical and physical adsorption as the adsorption mechanism between the SFM and the mild steel substrate. Polarization curves indicate that compound is mixed-type inhibitor, affecting both cathodic and anodic corrosion currents. The morphological study indicated adsorption of inhibitor molecules on the surface of the mild steel. The density functional theory (DFT) was employed for theoretical calculations. The results obtained from experimental measurements and those from theoretical calculations are in good agreement.

Keywords: Mild steel; DFT; Acid corrosion; EIS; SEM

INTRODUCTION

Mild steel is an important material which finds wide applications in industry due to its excellent mechanical properties and low cost[1]–[4]. It is extensively used in various industries as construction material for chemical reactors, heat exchanger and boiler systems, storage tanks, and oil and gas transport pipelines. To minimize the metal loss, corrosion inhibition programs are required[5]–[8]. The corrosion inhibition is achieved by the addition of inhibitor to the system that prevents corrosion of the metal surface.

The influence of the inhibitor upon metal corrosion is often associated with physical or chemical adsorption. This phenomenon is related to the presence of hetero atoms (N, O, and S) as well as multiple bonds or aromatic rings in the inhibitor[9]–[11]. Availability of non-bonded (lone pair) and π-electrons in inhibitor molecules facilitates electron transfer from the inhibitor to the metal. A coordinate covalent bond involving transfer of electrons from inhibitor to the metal surface may be formed[12]–[15]

The correlation between the inhibitor efficiency and the molecular structure of organic compounds has been extensively investigated[16]–[18]. The theoretical study of the inhibition efficiency of this SFM was carried out by DFT method. They found a close correlation between quantum mechanical parameters such as energy gaps, and dipole moment and inhibition efficiency of the compound.

The objective of this work is to investigate the corrosion inhibition properties of SFM, namely SFM on mild steel in 1.0 M HCl using electrochemical techniques, weight loss, and quantum chemical calculations. The schematic representation of the structure is presented in Fig. 1.

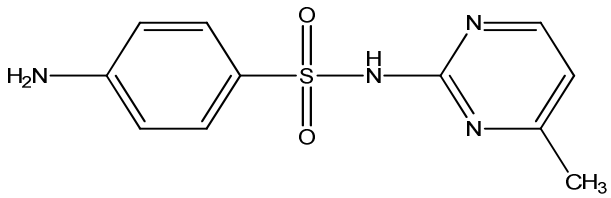

Fig. 1 Chemical structure of Sulfamerazine

MATERIALS AND METHODS

2.1. Electrodes and chemicals and test solution

Corrosion tests have been performed, using the gravimetric and electrochemical measurements, on electrodes cut from sheets of carbon steel with the chemical composition: 0.370 % C, 0.230 % Si, 0.680 % Mn, 0.016 % S, 0.077 % Cr, 0.011 % Ti, 0.059 % Ni, 0.009 % Co, 0.160 % Cu, and the remainder iron.

The aggressive medium of molar hydrochloric acid used for all studies were prepared by dilution of analytical grade 37% HCl with double distilled water. The concentrations of SFM used in this investigates were varied from 0.0001 to 0.005M.

2.2. Gravimetric measurements

Gravimetric measurements were realized in a double walled glass cell equipped with a thermostat-cooling condenser. The carbon steel specimens used have a rectangular form with dimension of 2.5 × 2.0 × 0.2 cm were abraded with a different grade of emery paper (320-800-1200) and then washed thoroughly with distilled water and acetone. After weighing accurately, the specimens were immersed in beakers which contained 100 ml acid solutions without and with various concentrations of SFM at temperature equal to 303 K remained by a water thermostat for 6h as immersion time. The gravimetric tests were performed by triplicate at same conditions.

The corrosion rates (C_R) and the inhibition efficiency ($\eta_{wt}\%$) of carbon steel have been evaluated from mass loss measurement using the following equations:

$$C_R = \frac{w}{St} \qquad (1)$$

$$\eta_{wt}\% = \frac{C_R^o - C_R}{C_R^o} \times 100 \qquad (2)$$

Where w is the average weight loss before and after exposure, respectively, S is the surface area of sample, t is the exposure time, C_R^o and C_R is the corrosion rates of steel without and with the SFM inhibitor, respectively.

2.3. Electrochemical tests

The potentiodynamic polarization curves were conducted using an electrochemical measurement system PGZ 100 Potentiostat/Galvanostat controlled by a PC supported by the Voltamaster 4.0 Software. The electrochemical measurements were performed in a conventional three electrode glass cell with carbon steel as a working electrode, platinum as counter electrode (Pt) and a saturated calomel electrode used as a reference electrode. The working electrode surface was prepared as described above gravimetric section. Prior to each electrochemical test an immersion time of 30 min was given to allow the stabilization system at corrosion potential. The polarization curves were obtained by changing the electrode potential automatically from -800 to -200 mV/SCE at a scan rate of 1 mV s-1. The temperature is thermostatically controlled at desired temperature ±1K.The percentage protection efficiency ($\eta_P\%$) is defined as:

$$\eta_P\ (\%) = \frac{I^0_{corr} - I_{corr}}{I^0_{corr}} \times 100 \quad (3)$$

Where, I^o_{corr} are corrosion current in the absence of inhibitor, Icorr are corrosion current in the presence of inhibitor. Electrochemical impedance spectroscopy (EIS) measurements were carried out with same equipment used for potentiodynamic polarization study (Voltalab PGZ 100) at applied sinusoidal potential waves of 5mV amplitudes with frequencies ranging from 100 KHz to 10 mHz at corrosion potential. The impedance diagrams are given in the Nyquist representation. The charge transfer resistance (R_{ct}) was determined from Nyquist plots and double layer capacitance (Cdl) was calculated from CPE parameters of the equivalent circuit deduced using Zview software. In this case the percentage protection efficiency (η_Z%) is can be calculated by the value of the charge transfer resistance (R_{ct})

$$\eta_Z\ (\%) = \frac{R_{ct} - R^0_{ct}}{R_{ct}} \times 100 \quad (4)$$

WhereR^o_{ct} and Rct were the polarization resistance of uninhibited and inhibited solutions, respectively.

2.4. density functional theory (DFT) method

Quantum chemical method is usually used to investigate the relationship between the inhibitor molecular properties and its corrosion inhibition efficiency[17], [18]. The properties include orbital energy, charge density and combined energy, etc.[19]. Some studies have investigated the correlation between the inhibitor molecular structure and its efficiency, but much less attention has been paid to simulate the adsorption mode of the inhibitor and the metal. Quantum chemical calculations were performed using density functional theory (DFT) with the Beck's three parameter exchange functional along with the Lee-Yang-Parr non local correlation functional (B3LYP)[20], [21] with 6-31G (d, p) basis set is implemented in Gaussian 03 program package[22]. This approach is shown to yield favorable geometries for a wide variety of systems. The following quantum chemical parameters were evaluated from the optimized molecular structure: the dipole moment (μ), the energy of the highest occupied molecular orbital (E_{HOMO}), the energy of the lowest unoccupied molecular orbital (E_{LUMO}), the energy band gap ($\Delta E_{gap} = E_{HOMO} - E_{LUMO}$), the electron affinity (A), the ionization potential (I) and the number of transferred electrons (ΔN).

RESULTS AND DISCUSSION

3.1. Polarization results

The corrosion of mild steel electrode in 1.0 M HCl solutions containing various concentrations of sulphonamide derivative was studied by potentiodynamic polarization. Inhibition efficiency η_p(%) was calculated by applying a relationship described in Eq. (3). Typical potentiodynamic polarization curves for mild steel in 1.MHCl in the absence and presence of different concentration of inhibitor are shown in Fig. 2, while the electrochemical parameters derived from the polarization curves are summarized in Table 1.

It is reported[23]that if the shift in corrosion potential exceeds ±85 mV with respect to corrosion potential of the uninhibited solution, the inhibitor acts as either anodic or cathodic type, the shift in E_{corr} values of the inhibited systems compared to the acid blank is less than 80 mV, suggesting that the studied compoundis mixed type inhibitor[17], [24].

Table 1. Polarization data of carbon steel in 1.0 M HCl without and with various concentrations of SFM at 303 K

Inhibitor	Conc (M)	$-E_{corr}$ (mV/SCE)	-βc (mV dec^{-1})	I_{corr} (μA cm^{-2})	η_{Tafel} (%)	Θ
Blank	-	496	162	564.0	-	-
SFM	5.10^{-3}	474	176	36.17	93.59	0.9359
	1.10^{-3}	478	167	45.84	91.87	0.9187
	5.10^{-4}	470	183	87.22	84.54	0.8454
	1.10^{-4}	473	169	137.36	75.65	0.7565

That is, they inhibit both the anodic dissolution of mild steel and the cathodic H^+ ion reduction[18], [25]. The values of the cathodic (βc) Tafel slope do not show any uniform trend, which again confirms mixed type inhibition mechanism of the studied sulphonamide derivative[26].The decrease of the corresponding current densities with increasing inhibitor concentration is due to the formation of anodic protective films on the electrode surface[27].

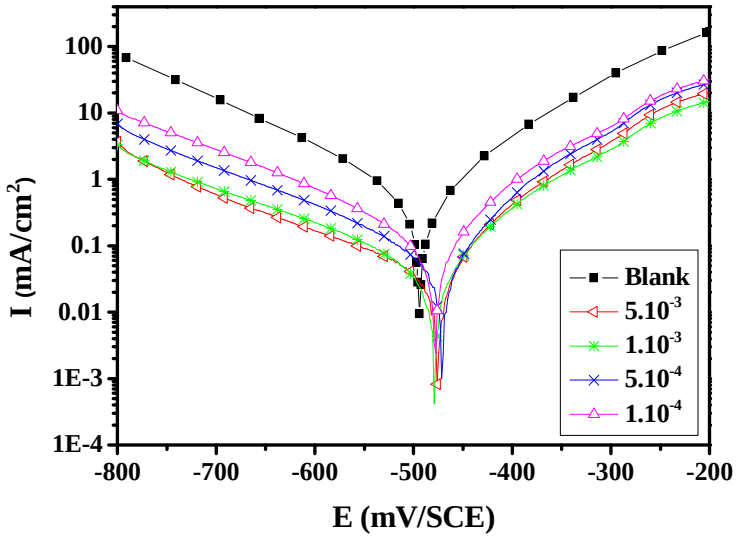

Fig. 2.Polarisation curves of carbon steel in 1.0 M HCl for various concentrations of SFM at 303K

3.2. Electrochemical impedance spectroscopy measurements

Electrochemical impedance measurements were undertaken to provide information on the kinetics of the electrochemical processes at the mild steel/acid interface and how this is modified by thepresence of inhibitor[28]. Nyquist plots for mild steel corrosion in 1.0 M HCl solution in the absence and presence of different concentrations of the inhibitor is given in Fig. 3, the impedance parameters deduced from the analysis of Nyquist diagram and values of ηz (%) are given in Table 2. As it can be seen, the impedance response of mild steel in uninhibited solution has significantly changed after the addition of SFM. Double layer capacitance values (C_{dl}) and charge-transfer resistance values (Rct) were obtained from impedance measurements. The double layer capacitance values (C_{dl}) is evaluated from constant phase element CPE (Q, n) and a charge transfer resistance value (Rct), using the following relation:

$$C_{dl} = \sqrt[n]{Q.R_t^{1-n}} \quad (5)$$

Where Q is the constant phase element (CPE) and n is a coefficient can be used as a measure of surface inhomogeneity.

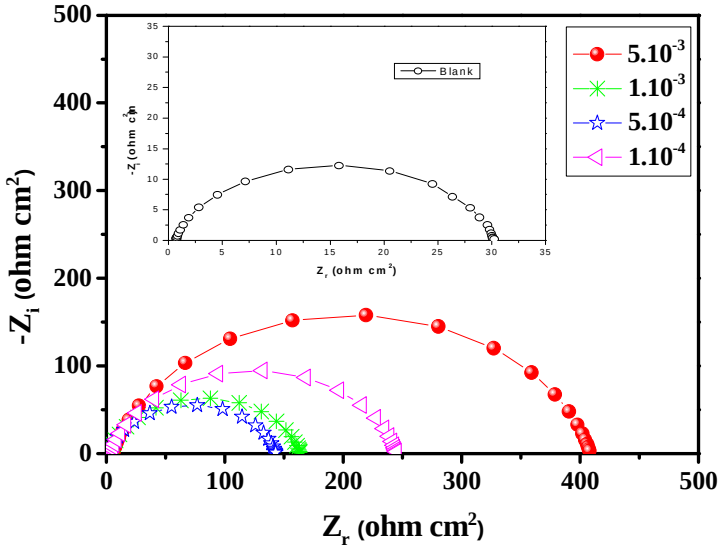

Fig. 3.Nyquist diagrams for carbon steel in 1.0 M HCl containing different concentrations of SFM at 303 K

Table 2. Impedance parameters for corrosion of carbon steel in 1.0 M HCl in the absence and presence of different concentrations of SFM at 303 K

Inhibitor	Conc (M)	R_{ct} (Ω cm^2)	n	$Q\times10^{-4}$ (s^n $\Omega^{-1}cm^{-2}$)	C_{dl} (μF cm^{-2})	η_z (%)	Θ
Blank	-	29 .35	0.91	1.7610	91.63	-	-
SFM	5.10^{-3}	403.00	0.81	0.2876	10.11	92.72	0.9272
	1.10^{-3}	244.75	0.79	0.4376	13.10	88.01	0.8801
	5.10^{-4}	162.87	0.82	0.8912	35.19	81.98	0.8198
	1.10^{-4}	141.08	0.80	1.0978	38.78	79.20	0.7920

By increasing the inhibitor concentration,Rct value increased. A large R_{ct} has associated with a slower corroding system. Furthermore, better protection provided by an inhibitor could be associated with a decrease in capacitance of the metal[29], [30]. Suitable equivalent circuit is used to simulate the impedance data in the presence of SFM as shown in Fig. 4, The introduction of CPE into the circuit was necessitated to explain the depression of the capacitance semicircle, which corresponds to surface heterogeneity resulting from surface roughness, impurities, and adsorption of inhibitor[31]. The impedance of this element is frequency-dependent and can be calculated using the Eq. 6[32]:

$$Z_{CPE} = \frac{1}{Q(j\omega)^n} \quad (6)$$

Where Q is the CPE constant (in $\Omega^{-1}S^n$ cm^{-2}), ω is the angular frequency (in rad s^{-1}), j2 = -1 is the imaginary number and n is a CPE exponent which can be used as a gauge for the heterogeneity or roughness of the surface.

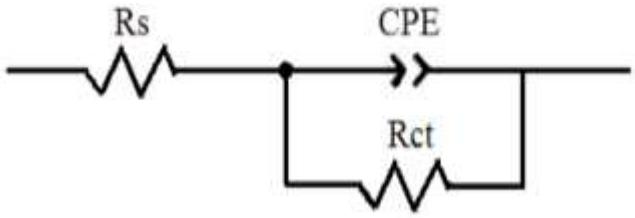

Fig. 4.Equivalent electrical circuit corresponding to the corrosion process on the carbon steel in hydrochloric acid

3.3. Weight loss tests

Corrosion parameters namely, corrosion rate (C_R), surface coverage (θ) and inhibition efficiency (η %) of mild steel in 1.0 MHCl solution in the absence and presence of different concentrations of inhibitor at 303 K, obtained from weight loss measurements are shown in Table 3and Fig. 5. From Table 3, and Fig. 5 it is apparent that inhibition efficiency increased with increasing the concentration of the inhibitor. The inhibition efficiency of SFM at 5.10^{-3} M was found to be 94.19, at 303 K (Table 3). The increase in inhibition efficiency and decrease in the corrosion rate with increasing concentration of inhibitor is due to increase in the surface coverage, resulting retardation of metal dissolution[33].

Table 3. Corrosion parameters obtained from weight loss measurements for carbon steel in 1.0 M HCl containing various concentration of SFM at 303 K

Inhibitor	Concentration (M)	C_R (mg cm^{-2} h^{-1})	η_w (%)	Θ
Blank	-	1.135	-	-
SFM	5.10^{-3}	0.066	94.19	0.9419
	1.10^{-3}	0.109	90.43	0.9043
	5.10^{-4}	0.176	84.52	0.8452
	1.10^{-4}	0.239	78.96	0.7896

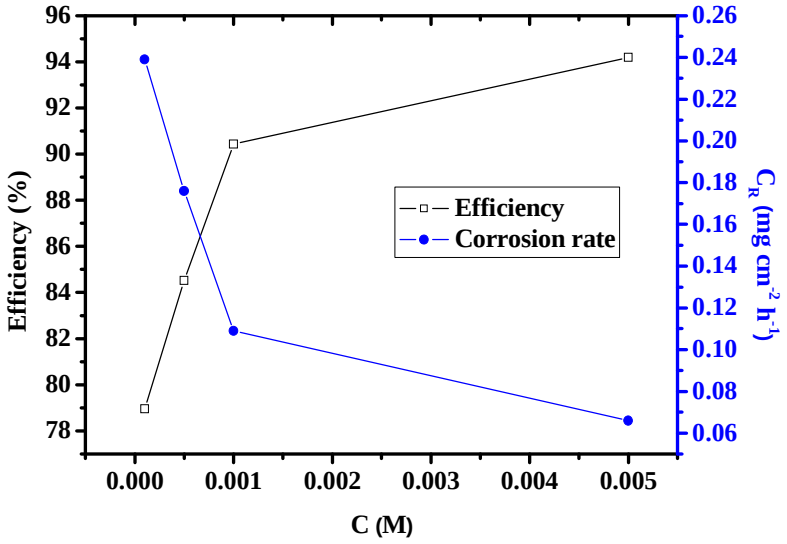

Fig. 5.Relationship between the corrosion rate, the inhibition efficiency and SFM concentrations for steel after 6 h immersion in 1.0 M HCl at 303 K

3.4. Effect of temperature

The effect of temperature on the inhibited acid–metal reaction is very complex, because many changes occur on the metal surface such as rapid etching, desorption of inhibitor and the inhibitor itself may undergo decomposition. The change of the I_{corr} at selected concentrations of SFM at different temperatures (303–333 K) was studied in 1.0 M HCl, both in the absence and presence of SFM using Tafel polarization technique. Inspection of the results obtained reveals that the corrosion rate increases with increasing the temperature both in uninhibited and inhibited conditions, the inhibition efficiency of SFM decreases on increasing solution temperature; these results suggest that the temperature can modify the interaction between the mild steel electrode and the acidic medium in the absence and in the presence of the inhibitor[34]–[36].

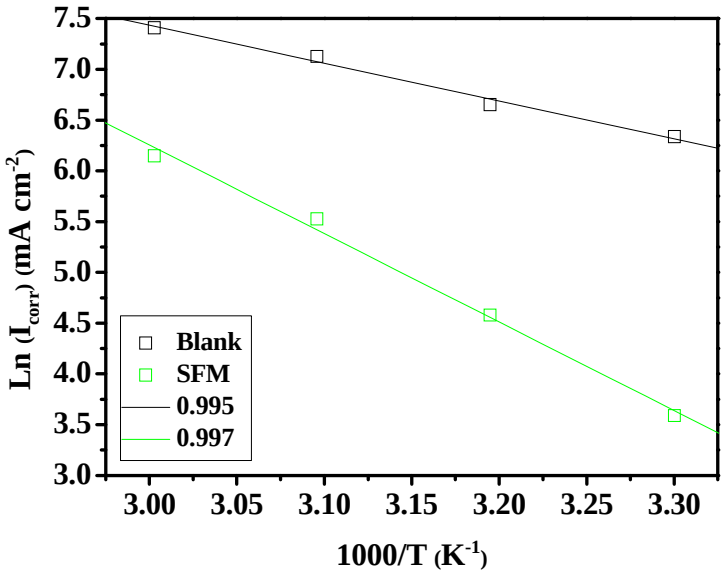

Figure 6. Arrhenius plots for mild steel in 1.0 M HCl and 1.0 M HCl + 5.10^{-3} M SFM

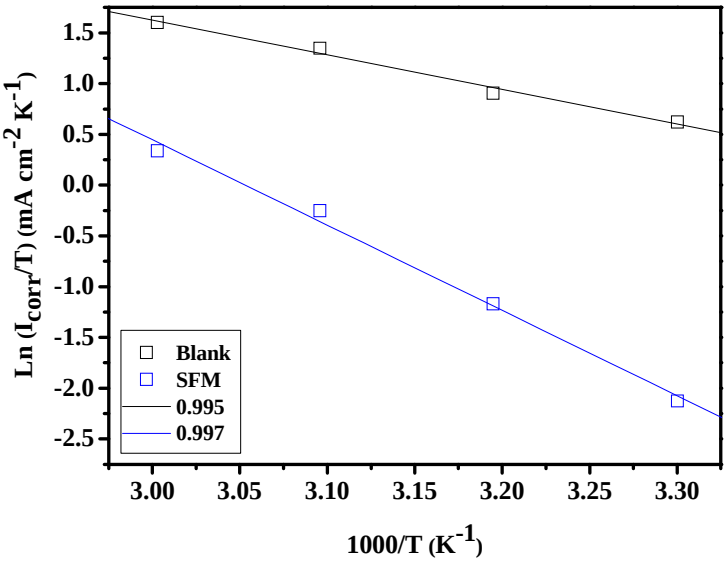

Fig. 7. Transition state plots for mild steel in 1.0 M HCl and 1.0 M HCl + 5.10^{-3} M SFM

In order to calculate the activation energy for the corrosion reaction, the Arrhenius Eq. 7 was used[29], [30]:

$$C_R = k\ exp\left(\frac{-E_a}{RT}\right) \qquad (7)$$

Where C_R is the corrosion rate, R the gas constant, T the absolute temperature, A the pre-exponential factor, The apparent activation energies (E_a) and pre-exponential factors (k) at 5.10^{-3} Mof inhibitor are calculated by linear regression between ln (I_{corr}) and 1/T (Fig.6), and also the results shown in Table 5. The linear regression coefficientis close to 1, indicating that the mild steel corrosion in hydrochloric acid can be elucidated using the kinetic model.It is evident from Table 5 that the value of the apparent activation energy for the inhibited solution were higher than that for the uninhibited solution, indicating that the dissolution of mild steel was decreased due to formation of a barrier by the adsorption of the inhibitor on metal surface[37], [39].

Table 4.The influence of temperature on the electrochemical parameters for carbon steel electrode immersed in 1.0 M HCl and 1.0 M HCl + 5.10^{-3} M SFM

Inhibitor	Temp (K)	**-E_{corr} (mV/SCE)**	**-βc (mV dec^{-1})**	**I_{corr} (µA cm^{-2})**	**η_{Tafel} (%)**
Blank	303	496	162.5	564	-
	313	498	154.5	773	-
	323	492	176.0	1244	-
	333	497	192.0	1650	-
SFM	303	474	176.0	36.17	**93.59**
	313	475	170.2	97.25	**87.42**
	323	468	168.23	250.87	**79.83**
	333	470	179.62	467.45	**71.67**

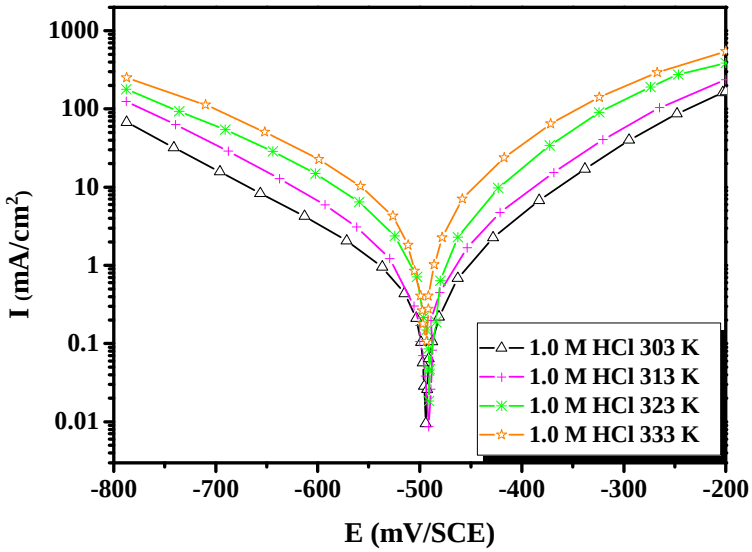

Fig. 8.Potentiodynamicpolarisation curves of carbon steel in 1.0 M HCl at different temperatures

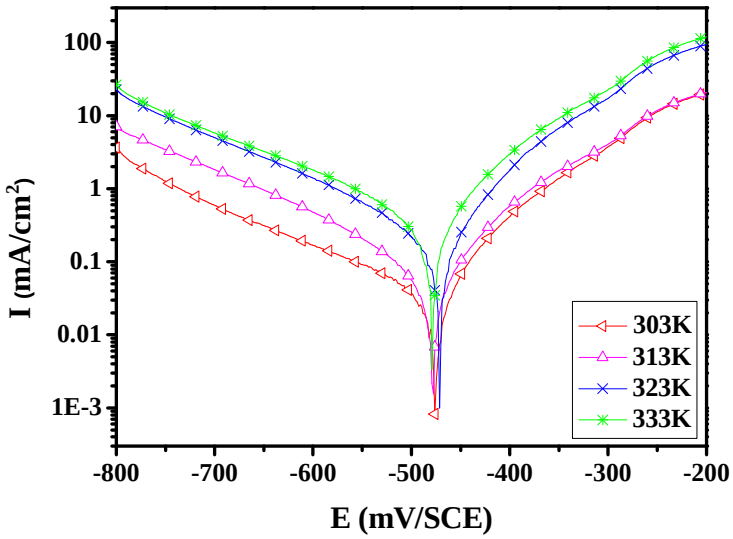

Fig. 9.Potentiodynamicpolarisation curves of carbon steel in 1.0 M HCl in the presence of 5.10^{-3} M SFM at different temperatures

Other activation parameters can be evaluated from the effect of temperature. Enthalpy and entropy of activation were calculated using the alternative form of Arrhenius[40], [41]Eq. 8:

$$C_R = \frac{RT}{Nh}\, exp\left(\frac{\Delta S_a}{R}\right) exp\left(-\frac{\Delta H_a}{RT}\right) \qquad (8)$$

Where, h is the Planck's constant, N is the Avogadro's number, R is the molar gas constant and T is the absolute temperature. Straight lines were obtained with a slope and an intercept (Fig. 7) from which the activation thermodynamic parameters ΔHa and ΔSa were calculated, as listed in Table 5. The values of Ea and ΔH are close to each other, as expected from the concept of transition-state theory, and follow the same pattern of variation with different concentrations of the inhibitor. The negative value of ΔS for inhibitor indicate that the formation of the activated complex in the rate determining step represents an association rather than a dissociation step, meaning that a decrease in disorder takes place during the course of the transition from reactants to activated complex[42], [43].

Table 5.Corrosion kinetic parameters for mild steel in 1.0 M HCl in the presence and absence of 5.10^{-3} M SFM

Inhibitor	E_a (kJ/mol)	ΔH_a (kJ/mol)	ΔS_a (J mol-1 K-1)	$E_a - \Delta H_a$
Blank	31.00	28.35	-98.8	2.65
SFM	72.46	69.83	15.83	2.63

3.5. Adsorption considerations

The adsorption of organic molecules provides information about the interaction among the adsorbed molecules themselves as well as their interaction with the electrode surface.Tafel polarization technique is employed to find out the values of surface coverage θ at different inhibitor concentrations, these values are used to explain the best fit isotherm to determine the adsorption process. Data are tested graphically by fitting to various isotherms. In the temperature range studied, the best correlation between the experimental results and the isotherm function is obtained using Langmuir's adsorption isotherm.Langmuir's adsorption isotherm is given by the Eq. (9)

$$\frac{C_{inh}}{\theta} = \frac{1}{K_{ads}} + C_{inh} \qquad (9)$$

Where, C is the concentration of the inhibitor, Kads is the equilibrium constant of adsorption and θ is the surface coverage.

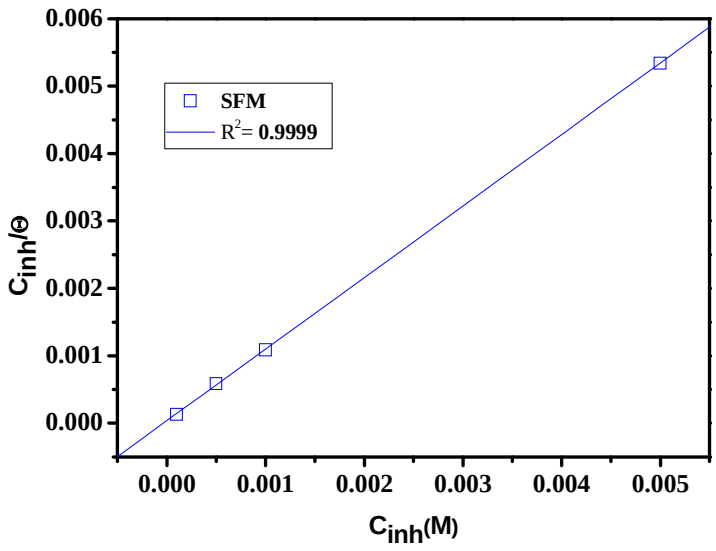

Fig. 10.Langmuir adsorption of SFM on the carbon steel surface in 1.0 M HCl solution at 303K

Table 5. Thermodynamic parameters for the adsorption of SFM in 1.0 M HCl on the Carbon steel at 303K

Inhibitor	Slope	$K_{ads}(M^{-1})$	$\Delta G°_{ads}$(kJ/mol)
SFM	1.0626105.33	**5.72**	

The value of K is related to the standard free energy of adsorption, $\Delta G°_{ads}$, by the following equation:

$$\Delta G^0_{ads} = -RTln(K * 55.5) \qquad (10)$$

Where the value 55.5 is the water concentration in solution expressed in $mol.L^{-1}$.

The values of adsorption constant, slope, and linear correlation coefficient (R^2) can be obtained from the regressions between C/θ and C, (Fig.10) and the results are listed in Table 5. The result shows that the linear correlation coefficient and the slope are close to one and confirm that the adsorption of SFM in 1.0 M HCl follows the Langmuir adsorption isotherm.The negative values of ΔG_{ads} ensure the spontaneity of adsorption process and stability of the adsorbed layer on the metal surface[44], [45]. Generally, values of (ΔG_{ads}) up to −20 kJ/mol are consistent with the electrostatic interactions between the charged molecules and the charged metal (physisorption) while those around −40 kJ/mol or higher are associated with chemisorption as a result of sharing or transfer of electrons from polymer molecules to the metal surface to form a coordinate type of bond (chemisorption). The value

of ΔG_{ads} listed in Table 5 indicate the both chemisorption and physisorption of SFM on the mild steel surface[40], [46], [47].

3.6. Quantum Chemical Calculations

Quantum chemical calculations are utilized to ascertain whether there is a clear relationship between the molecular structure of the SFM inhibitor and its inhibition effect. The structure parameters of the SFM inhibitor are used to elucidate the inhibition mechanism in the present work. The equilibrium geometry structures and the frontier molecule orbital density distributions of the molecule are shown in Fig. 11 and the quantum chemical parameters are listed in Table 6.

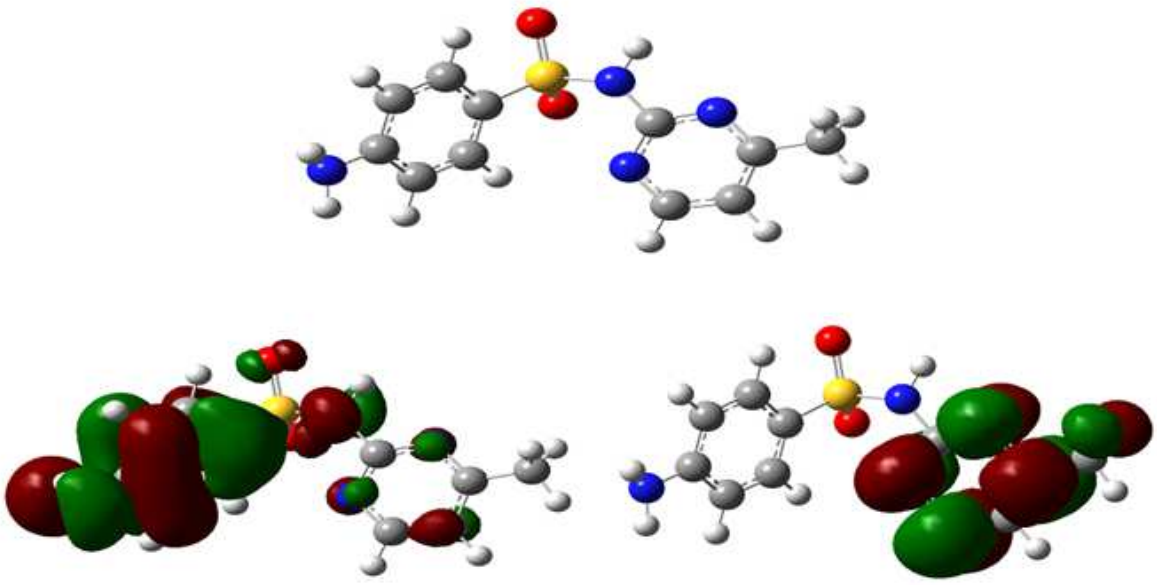

Figure11. Optimized structures and Frontier molecular orbital density distributions HOMO (left) and LUMO (right) of SFM

From Table6, the high value of dipole moment probably increases the adsorption between chemical compound and metal surface [44]. The adsorption of SFM molecules from the aqueous solution can be regarded as a quasi-substitution process between the SFM in the aqueous phase [SFM (sol)] and water molecules at the electrode surface [H_2O (ads)].

E_{HOMO} is often associated with the capacity of a molecule to donate electron. High value of E_{HOMO} probably indicates a tendency of the molecule to donate electrons to appropriate acceptor molecules with low energy and empty molecular orbital. E_{LUMO} indicates the ability of the molecule toaccept electrons. The lower the value of E_{LUMO}, the more probable is that the molecule would accept electrons [45]. According to frontier orbital theory, the reaction of reactants mainly occurs on HOMO and LUMO [46]. From Table 6, the high value of E_{HOMO} (-5.93317eV) is likely to indicate a tendency to donate electrons to appropriate low-energy acceptor states. Increasing values of the E_{HOMO} facilitate adsorption (and therefore inhibition) by influencing the transport process through the adsorbed layer. E_{LUMO} indicates the ability of the molecule to accept electrons; hence these are the acceptor states. The lower the value (-1.04954eV) of E_{LUMO}, the more probable it is that the molecule would accept electrons [47].

Another method to correlate inhibition efficiency with parameters of molecular structure is to calculate the fraction of electrons transferred from inhibitor to metal surface. According to Koopman's theorem [48], E_{HOMO} and E_{LUMO} of the inhibitor molecule are related to the ionization potential (I) and the electron affinity (A), respectively. The ionization potential (I) and the electron affinity (A) are defined as follows:

$$I = -E_{HOMO} \quad (11)$$

$$A = -E_{LUMO} \quad (12)$$

Then absolute electronegativity (χ) and global hardness (η) of the inhibitor molecule are approximated as follows [49]:

$$\chi = \frac{I + A}{2} \tag{13}$$

$$\eta = \frac{I - A}{2} \tag{14}$$

Thus the fraction of electrons transferred from the inhibitor to metallic surface, ΔN, is given by [50]:

$$\Delta N = \frac{\chi_{Fe} - \chi_{inh}}{2(\eta_{Fe} + \eta_{inh})} \tag{15}$$

To calculate the fraction of electrons transferred the theoretical values of χ_{Fe}(7 eV mol^{-1}) and of η_{Fe} (0 eV mol^{-1}) are used [51]. The calculated results are presented in Table 6.

Table 6.Calculated quantum chemical parameters of the studied compound

	μ (debye)	TE (eV)	E_{HOMO} (eV)	E_{LUMO}(eV)	ΔE_{gap}(eV)	χ (eV)	η (eV)	ΔN
SFM	7.1408	-32490	-5.93317	-1.04954	4.88363	3.491	2.442	0.718

Generally, value of ΔN shows inhibition efficiency resulting from electron donation, and the inhibition efficiency increases with the increase in electron-donating ability to the metal surface. Value of ΔN show inhibition effect resulted from electrons donation. According toLukovits's study [52], if ΔN < 3.6, the inhibition efficiency increases with increasing electron-donating ability at the metal surface.Based on these calculations, it is expected that the synthesized inhibitor is donor of electrons, and the steel surface is the acceptor, and this favors chemical adsorption of the inhibitor on the electrode surface. Here the inhibitor binds to the steel surface and forms an adsorption layer against corrosion. The SFM inhibitor shows the highest inhibition efficiency because it has the highest HOMO energy and this reflects the greatest ability of offering electrons. It can be seen from Table 6 that the ability of the inhibitor to donate electrons to the metal surface, which is in good agreement with the higher inhibition efficiency of the SFM inhibitor.

CONCLUSION

The following conclusions can be drawn from the studies.

- The Sulfamerazine show good inhibition efficiencies for the corrosion of mild steel in 1.0 MHCl solutions and the inhibition efficiency increases on increasing concentration of the inhibitor and decreases with increase in temperature.
- The variation in the values of βc (Tafel slope) and the minor displacement of E_{corr} with respect to E_{corr} of the blank indicate that the inhibitoris mixed type in nature.
- EIS measurements show that the charge transfer resistance (Rct) increases and the double layer capacitance (C_{dl}) decreases in the presence of the inhibitors which implied the adsorption of the inhibitor molecules on the mild steel surface.
- The adsorption of the inhibitor was found to be spontaneous and obey the Langmuir adsorption isotherm featuring competitive physisorption and chemisorption mechanisms.
- Quantum chemical calculations showed a good agreement between the theoretical and experimental results.

Acknowledgment
The authors would like to thank MENA NWC for their financial support for grant no: WIF 04. Also, we would like to extend our thanks to Palestine Water Authority (PWA) and MEDRIC for their support.The support given through an"INCRECYT" research contract to M. Zougagh is also acknowledged.

REFERENCES

[1] D. B. Hmamou, R. Salghi, A. Zarrouk, H. Zarrouk, M. Errami, B. Hammouti, L. Afia, L. Bazzi, et L. Bazzi, *Res. Chem. Intermed.*, **2013**, 39, 3, 973‑989,.
[2] M. Larouj, H. Lgaz, S. Houda, H. Zarrok, H. Bourazmi, A. Zarrouk, A. Elmidaoui, A. Guenbour, S. Boukhris, et H. Oudda, *J. Mater. Environ. Sci*, **2015**. 6 (11), 3251-3267

[3] L. Afia, R. Salghi, L. Bammou, E. Bazzi, B. Hammouti, L. Bazzi, et A. Bouyanzer, *J.SaudiChem.Soc.*, **2014**, 18, 19‑25.
[4] Lebrini, M., Bentiss, F., Chihib, N., Jama, C., Hornez, J. P., Lagrenée, M. *Corros. Sci*.**2008**, 50, 2914-2918.
[5] O. Ouachikh, A. Bouyanzer, M. Bouklah, J.-M.Desjobert, J. Costa, B. Hammouti, et L. Majidi, *Surf. Rev. Lett.*, **2009**, 16, 01, 49‑54,.
[6] L. Afia, R. Salghi, E. H. Bazzi, A. Zarrouk, B. Hammouti, M. Bouri, H. Zarrouk, L. Bazzi, et L. Bammou, *Res. Chem. Intermed.,* **2012**, 38, 8, 1707‑1717.
[7] D. B. Hmamou, R. Salghi, A. Zarrouk, O. Benali, F. Fadel, H. Zarrok, et B. Hammouti, *Int. J. Ind. Chem.,* **2012**, 3, 1, 1‑9.
[8] L. Afia, R. Salghi, A. Zarrouk, H. Zarrok, E. H. Bazzi, B. Hammouti, et M. Zougagh, *Trans. Indian Inst. Met.*, **2013**, 66, 1, 43‑49,.
[9] E. H. A. Addi, L. Bazzi, M. Hilali, E. A. Zine, R. Salghi, et S. E. Issami, *Can. J. Chem*.,**2003**, 81, 4, 297‑306,.
[10] A. Bousskri, A. Anejjar, M. Messali, R. Salghi, O. Benali, Y. Karzazi, S. Jodeh, M.Zougagh, E. E. Ebenso, et B. Hammouti, *J. Mol. Liq*., **2015**, 211, 1000‑1008.
[11] N. S. Patel, J. Hadlicka, P. Beranek, R. Salghi, H. Bouya, H. A. Ismat, et B. Hammouti, *Port. Electrochimica Acta,* **2014**, 32, 6, 395‑403.
[12] L. Bammou, M. Belkhaouda, R. Salghi, O. Benali, A. Zarrouk, H. Zarrok, et B.Hammouti, *J. Assoc. ArabUniv.* Basic Appl. Sci**., 2014**, 16, 83‑90.
[13] R. Salghi, L. Bazzi, B. Hammouti, S. Kertit, A. Bouchtart, et Z. El Alami, présenté àAnnales de Chimie Science des Materiaux, **2000**, 25, 593‑600.
[14] R. Salghi, L. Bazzi, B. Hammouti, S. Kertit, A. Bouchtart, et Z. El Alami, *Ann. Chim. Sci. Matér*., **2000**, 25, 8, 593‑600.
[15] R. Salghi, L. Bazzi, et M. Zaafrani, *Acta Chim. Slov*.,**2003**, 50, 3, 491‑504,.
[16] D. B. Hmamou, R. Salghi, A. Zarrouk, M. R. Aouad, O. Benali, H. Zarrok, M. Messali, B. Hammouti, M. M. Kabanda, et M. Bouachrine, *Ind. Eng. Chem. Res*., **2013**, 52, 40, 14315‑14327.
[17] R. N. Singh, A. Kumar, R. K. Tiwari, et P. Rawat, *Spectrochim. Acta. A. Mol. Biomol. Spectrosc*.**2013**, 112, 182‑190.
[18] H. Jafari, I. Danaee, H. Eskandari, et M. RashvandAvei, *J. Mater. Sci. Technol*., **2014**, 30, 3, 239‑252.
[19] L. M. Rodríguez-Valdez, W. Villamisar, M. Casales, J. G. González-Rodriguez, A.Martínez-Villafañe, L. Martinez, et D. Glossman-Mitnik, *Corros. Sci*., **2006**, 48, 12, 4053‑4064.
[20] A. D. Becke, *Phys. Rev. A*, **1988**, 38, 6, 3098‑3100.
[21] C. Lee, W. Yang, et R. G. Parr, *Phys. Rev. B*, **1988**, 37, 2, 785‑789.
[22] M. J. Frisch, G. W. Trucks, H. B. Schlegel, G. E. Scuseria, M. A. Robb, J. R. Cheeseman, J. A. Montgomery, Jr., T. Vreven, K. N. Kudin, J. C. Burant, J. M. Millam, S. S. Iyengar, J. Tomasi, V. Barone, B. Mennucci, M. Cossi, G. Scalmani, N. Rega, G. A.Petersson, H. Nakatsuji, M. Hada, M. Ehara, K. Toyota, R. Fukuda, J. Hasegawa, M. Ishida, T. Nakajima, Y. Honda, O. Kitao, H. Nakai, M. Klene, X. Li, J. E. Knox, H. P. Hratchian, J. B. Cross, V. Bakken, C. Adamo, J. Jaramillo, R. Gomperts, R. E. Stratmann, O.Yazyev, A. J. Austin, R. Cammi, C. Pomelli, J. W. Ochterski, P. Y. Ayala, K. Morokuma, G. A. Voth, P. Salvador, J. J. Dannenberg, V. G. Zakrzewski, S. Dapprich, A. D. Daniels, M. C. Strain, O. Farkas, D. K. Malick, A. D. Rabuck, K. Raghavachari, J. B. Foresman, J. V. Ortiz, Q. Cui, A. G. Baboul, S. Clifford, J. Cioslowski, B. B. Stefanov, G. Liu, A. Liashenko, P. Piskorz, I. Komaromi, R. L. Martin, D. J. Fox, T. Keith, M. A. Al-Laham, C. Y. Peng, A. Nanayakkara, M. Challacombe, P. M. W. Gill, B. Johnson, W. Chen, M. W. Wong, C. Gonzalez, and J. A. Pople, « Gaussian 03, Revision C.02 »,. Gaussian, Inc., Wallingford CT, **2004**.
[23] C. Verma, M. A. Quraishi, et A. Singh, *J. Mol. Liq*., **2015**, 212, 804‑812.
[24] C. Verma, E. E. Ebenso, I. Bahadur, I. B. Obot, et M. A. Quraishi, *J. Mol. Liq.,* **2015**, 212, 209‑218.
[25] C. Verma, M. A. Quraishi, et A. Singh, J. *Taiwan Inst. Chem. Eng*., **2016**, 58, 127‑140.
[26] D. Daoud, T. Douadi, H. Hamani, S. Chafaa, et M. Al-Noaimi, *Corros. Sci*., **2015**, 94,21‑37.
[27] M. V. Fiori-Bimbi, P. E. Alvarez, H. Vaca, et C. A. Gervasi, *Corros. Sci*., **2015**, 92, 192‑199.
[28] I. Lukovits, E. Kalman, et F. Zucchi, *Corrosion*, **2001**, 57, no 1, p. 3‑8.
[29] S. Kharchouf, L. Majidi, M. Bouklah, B. Hammouti, A. Bouyanzer, et A. Aouniti, *Arab. J. Chem*., **2014**. 7, 5, 680‑686.
[30] K. Ramya, R. Mohan, K. K. Anupama, et A. Joseph, *Mater. Chem. Phys*., **2015**,149‑150, p. 632‑647.
[31] I. B. Obot et A. Madhankumar, *J. Ind. Eng. Chem*., **2015**, 25, 105‑111.
[32] R. Yıldız, T. Doğan, et İ. Dehri, *Corros. Sci.,* **2014**,85, 215‑221.
[33] L. Feng, H. Yang, et F. Wang, *ElectrochimicaActa*, **2011**, 58, 427‑436.
[34] A. Biswas, S. Pal, et G. Udayabhanu, *Appl. Surf. Sci*., **2015**, 353, 173‑183.

[35] X. Li, S. Deng, et X. Xie, J. *Taiwan Inst. Chem. Eng*., **2014**, 45, 4, 1865‑1875.
[36] X. Li, S. Deng, et X. Xie, *Corros. Sci*., **2014**, 81, 162‑175.
[37] A. Khadiri, R. Saddik, K. Bekkouche, A. Aouniti, B. Hammouti, N. Benchat, M. Bouachrine, et R. Solmaz, J. *Taiwan Inst. Chem. Eng.*, **2016**, 58, 552‑564.
[38] H. Zarrok, A. Zarrouk, B. Hammouti, R. Salghi, C. Jama, et F. Bentiss, *Corros. Sci*., **2012**, 64,243‑252.
[39] Y. Sasikumar, A. S. Adekunle, L. O. Olasunkanmi, I. Bahadur, R. Baskar, M. M. Kabanda, I. B. Obot, et E. E. Ebenso, *J. Mol. Liq*., **2015**, 211, 105‑118.
[40] M. Mobinet M. Rizvi, *Carbohydr. Polym*.,**2016**, 136, 384‑393.
[41] N. A. Odewunmi, S. A. Umoren, Z. M. Gasem, S. A. Ganiyu, et Q. Muhammad, J.*Taiwan Inst. Chem. Eng*., **2015**, 51, 177‑185.
[42] Bouklah M., Benchat N., Aouniti A., Hammouti B., Benkaddour M., Lagrenée M., Vezin H., Bentiss, F., *Prog. Org. Coat* .**2004**, 51,118-124
[43] K. F. Khaled, *ElectrochimicaActa*, **2010**, 55, 22, 6523‑6532.
[44] N. A. Odewunmi, S. A. Umoren, et Z. M. Gasem, *J. Environ. Chem. Eng.*, **2015**, 3, 1, 286‑296.
[45] N. O. Eddy, H. Momoh-Yahaya, et E. E. Oguzie, *J. Adv. Res.*, **2015**, 6, 2, 203‑217.
[46] D. Zhang, Y. Tang, S. Qi, D. Dong, H. Cang, et G. Lu, *Corros. Sci*., **2016**, 102, 517‑522.
[47] M. H. Hussin, A. A. Rahim, M. N. Mohamad Ibrahim, et N. Brosse, *Measurement*, **2016**, 78, 90‑103.
[48] S. Vijayakumar, P. Kolandaivel, J. Mol. Struct. S. Vijayakumar, P. Kolandaivel*J. Mol...Struct*, **2006** 770 23-29.
[49] M. Bouklah, N. Benchat, B. Hammouti, A. Aouniti, S. Kertit, *Mater. Lett* ,**2006**, 60 1901.
[50] N. Khalil, *Electrochim. Acta*, **2003**, 48 2635.
[51] M. Lebrini, M. Lagrenee, M. Traisnel, L. Gengembre, H. Vezin, F. Bentiss, *Appl. Surf. Sci*, **2007**, 253 9267.
[52] G. Gece, *Corros. Sci*, **2008**, 50, 2981–2992.
[53] V.S. Sastri, J.R. Perumareddi, *Corrosion*, 1997, 53 671.
[54] R.G. Pearson, *Inorg. Chem*, **1988**, 27 734.
[55] S. Martinez, *Mater. Chem. Phys*, **2002**, 77 97.
[56] I. Lukovits, E. Kalman, F. Zucchi, *Corrosion*, **2001**, 57 3.